



Surface Science Letters

Effect of nitrogen incorporation and oxygen vacancy on electronic structure and the absence of a gap state in HfSiO films

Moon Hyung Jang ^{a,1}, Kwang Sik Jeong ^b, Kwun Bum Chung ^c, Jin Woo Lee ^d, Myeung Hee Lee ^e, Mann-Ho Cho ^{a,b,*}^a Atomic-scale Surface Science Research Institute, Yonsei University, Seoul 120-749, Republic of Korea^b Institute of Physics and Applied Physics, Yonsei University, Seoul 120-749, Republic of Korea^c Department of Physics, Dankook University, Cheonan 330-714, Republic of Korea^d LG Innotek, 379, Gasoo-Dong, Osan, 447-705, Republic of Korea^e Department of Physics, Yonsei University, Wonju 220-710, Republic of Korea

ARTICLE INFO

Article history:

Received 18 October 2011

Accepted 9 April 2012

Available online 20 April 2012

Keywords:

HfSiO

Ab-initio calculations

Medium energy ion scattering

Near-edge x-ray absorption fine structure

Reflection electron energy loss spectroscopy

Absence of gap state

ABSTRACT

The effect of nitrogen (N) incorporation into HfSiO on the electronic structure and band alignment of HfSiO films was investigated. N depth profile data obtained by medium energy ion scattering (MEIS) showed that the concentration of N or the bonding or electronic state of N in the film was stable when the film was annealed at 950 °C, while the oxygen (O) in HfSiON films was present in dissociated form, as evidenced by the unoccupied electronic state of O. The valence band offsets of the HfSiO films were strongly affected by N incorporation due to the presence of N in a 2p state. Moreover, a reduction in the conduction band offset of a HfSiO film was confirmed after the film was annealed in an atmosphere of N₂. The unoccupied state of the O vacancy is responsible for the change in the conduction band offset. The results of *ab-initio* calculations for the density of states (DOS) of HfSiO and HfSiON supercells were in agreement with the experimental results. The incorporation of N into HfSiO prevents the formation of a gap-state inside the band gap despite the fact that an O vacancy is generated in the film.

© 2012 Elsevier B.V. All rights reserved.

HfSiO has been investigated as a gate dielectric, in an attempt to improve the mobility at the interface and the structural stability of HfO₂. However, a survey of the literature indicates that HfSiO films are separated into two phases comprised HfO₂ and SiO₂ at temperatures above 900 °C, due to the high chemical potential [1]. One possible solution for eliminating this phase separation problem is the nitridation of HfSiO, since it would reduce the difference in the chemical potential of HfO₂/SiO₂, passivate dangling bonds at the interface and block the penetration of dopants. In practical device fabrication processes, post nitridation annealing (PNA) is typically used to increase the density of the film and to reduce leakage current, which originates from trap sites [2,3]. The conduction band offset (ΔE_c) and the valence band offset (ΔE_v) between the dielectric and channel materials have recently been examined, since band alignment has a critical effect on leakage current, which is caused by Schottky emission [4]. Although a number of research groups have investigated the band alignment of HfSiO as a function of N incorporation, there are only a few experimental and theoretical results available concerning the electronic state and the

band structure of HfSiON films prepared using various PNA conditions [5].

The focus of this study was to clarify the origin of changes in the electronic state and the band gap (E_g) and the band offset of HfSiO using PNA conditions that are actually employed in the fabrication process [6]. HfSiO films were deposited on *p*-type Si (100) substrates in 10 Å-thick SiO₂ layers by atomic layer deposition (ALD) at 300 °C. Nitridation and sequential post annealing treatments were performed to investigate the effect of PNA on the physical properties and the band alignment of HfSiO as follows: (1) Nitridation of the as-grown film was performed in a NH₃ atmosphere for 60 s at 750 °C (RTN) (2). After the RTN process, the film was sequentially annealed in a N₂ atmosphere for 30 s at 950 °C (RTNA). The depth profile of the HfSiO films was determined by MEIS using a 100 keV proton beam in a double alignment geometry. Near edge x-ray absorption fine structure (NEXAFS) O/N K-edge spectra were obtained at the 7B1 beamline at the Pohang acceleration laboratory (PAL). N 1s core level and valence spectra were obtained by x-ray photoelectron spectroscopy (XPS). Reflection electron energy loss spectroscopy (REELS) spectra were obtained using a VG ESCALAB 210 apparatus with a primary energy of 1000 eV.

The *ab-initio* calculations were performed for the following systems: (1) HfSiO and (2) HfSiON without an O vacancy and (3) HfSiO and (4) HfSiON with O vacancies (neutral, positively charged and negatively charged vacancy: V⁰, V⁺, V²⁺, V⁻ and V²⁻) to confirm

* Corresponding author at: Institute of Physics and Applied Physics, Yonsei University, Seoul 120-749, Republic of Korea.

E-mail address: mh.cho@yonsei.ac.kr (M.-H. Cho).

¹ Current address: Department of Materials Science and Engineering, University of Pennsylvania, Philadelphia, PA 19104, USA.

the effect of incorporated N and the O vacancies in the HfSiO and HfSiON films. It is important to determine the extent of the charged O vacancy because these defects affect the conduction process that occurs via electrons or holes [7]. The supercells contained 24, 48, 95 and 191 atoms in the cases of (1) $\text{Hf}_4\text{Si}_4\text{O}_{16}$, (2) $\text{Hf}_8\text{Si}_8\text{O}_{28}\text{N}_4$, (3) $\text{Hf}_{16}\text{Si}_{16}\text{O}_{63}$ and (4) $\text{Hf}_{32}\text{Si}_{32}\text{O}_{111}\text{N}_{16}$, respectively. In the cases of N incorporation, N is located substitutionally on O site. It was necessary to increase the size of the supercells to permit only one O vacancy to be generated in (3) and (4). Since these supercells have been verified in numerous previous studies, it would be very useful to analyze the experimental behavior of the HfSiO films using *ab-initio* calculations [8]. The total energy and the density of the states were calculated using the Vienna Ab-initio Simulation Package (VASP) [9]. To optimize the total energies and geometry using pseudopotentials, a plane-wave cutoff energy of 450 eV with the Perdew, Burke, Ernzerhof (PBE) exchange–correlation functional of the generalized gradient approximation (GGA) was used. The electronic states were calculated after geometrical optimization using the same PBE functional with a plane-wave cutoff energy of 500 eV. Three-dimensional atomistic visualizations were carried out using VESTA code [10].

Fig. 1 shows MEIS depth profiles determined by fitting the raw data. The raw data with the fitting results are shown in supplementary material (Fig. S1) [11]. The Hf to Si ratio was about 1.0 at the interfacial region, while it was about 1.3 at the surface region of an as-grown film. After the RTN process, as shown in Fig. 1(b), the total number of N atoms in the entire film appeared to be 25.9% of the total number of O atoms in an as-grown film. In the mean time, the total number of O atoms decreased by about 29.2% compared to that for an as-grown film, indicating that N readily substitutes for O in the film, in spite of the fact that there is a 3.3% difference between them. Previous reports showed that most of the N reacts with SiO_2 in HfSiO, resulting in the formation of chemical bonds such as $\text{N}=\text{Si}_3$ and $\text{Si}-\text{O}-\text{N}$. The reaction process between N and SiO_2 is based on the exchange process of O in the SiO_2 by N [12,13]. The tendency for N depth profiling is almost the same as the Si profiling in MEIS spectra, which is consistent with the reaction process. In RTNA films, the depth distribution of N was similar to that of Si because N forms a

more stable bond with Si. Since Si segregation occurs on the surface of the HfSiO film when the annealing is done at a temperature of over 900 °C, the concentration of Hf becomes increased by 2 nm–5 nm in the depth region [1]. Although a slight segregation of Si in the surface direction was observed due to the phase separation, the change in the concentration of Si and N was minimal after the RTNA, which results in a stable stoichiometry in the depth direction.

The K edge spectra of O and N were obtained using NEXAFS to verify the unoccupied states of O and N. The chemical states of N in the RTN and RTNA films were also examined using XPS N 1s core level spectra. Fig. 2(a) and (b) shows K edge NEXAFS spectra for O and N for different annealing conditions. These are related to ($\text{Hf } 5d + \text{O } (N) 2p$), ($\text{Hf } 6sp + \text{O } (N) 2p$), and ($\text{Si } 3sp + \text{O } (N) 2p$) states in the HfSiON films [14]. After nitridation, the intensity of the O K edge was decreased because N was substituted by O. We also observed that the energy difference between shoulder and the main peak is almost the same in the NEXAFS spectra for both the K edge of N and O because of the substitutional exchange of O by N. Moreover, the peak shape for O remains unchanged after the RTNA, except for a change in intensity. This indicates that nitridation suppresses changes in the electronic structure of O by randomized interaction between π -bonding states [15]. In addition, the change in the intensity of the O peak indicates that an O vacancy is generated in the RTNA film during the annealing treatment because distorted O

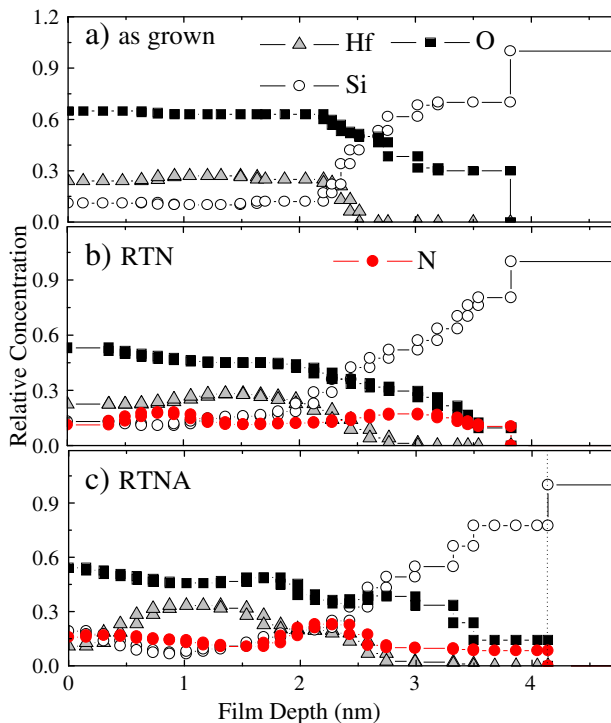


Fig. 1. MEIS depth profiling data for (a) as-grown, (b) RTN and (c) RTNA films.

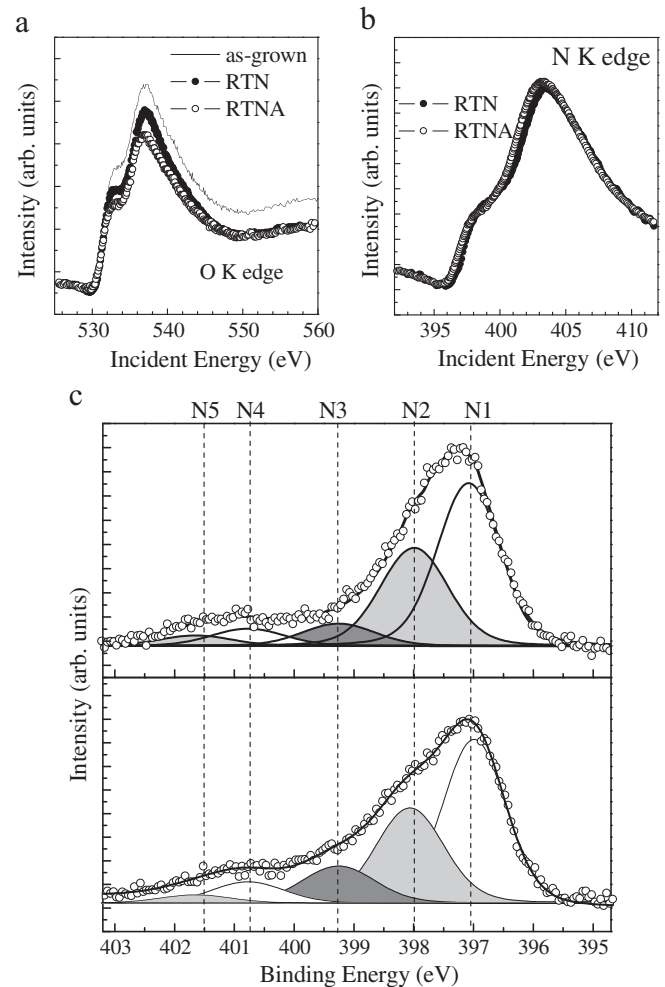


Fig. 2. (a) K edge NEXAFS spectra of O in an as-grown film, an RTN film and an RTNA film. (b) N K edge NEXAFS spectra of RTN and RTNA films. (c) N 1s XPS core level spectra of RTN and RTNA films. Open circles denote the raw data and the solid line superimposed on the raw data represent the results for the convolution of the fitted components (lines).

bonding in nitrated SiO₂ structure is dissociated at the high annealing temperature. In Fig. 2(b), the peak shape and intensity of the K edge spectra of N for RTN and RTNA are almost the same, indicating that their electronic structure was not significantly altered by the RTNA process.

The XPS N 1s spectra (open circles) in Fig. 2(c) were deconvoluted with several N chemical states of N1 to N5. Except for the N1 and N5 lines, no significant changes in intensity were evident. Based on the peak position of N 1s for HfSiO_xN_y (Hf–N=Si₂) and Si₃N₄ (N≡Si₃) at 396.8 and 397.8 eV, respectively, the N1 line at about 397.3 eV is presumably due to a N component related to Si-rich HfSiO_xN_y [12,13]. In addition, as discussed above, the concentration of N has a tendency to follow that of Si. Therefore, this core level state is estimated to be in a Si-rich HfSiO_xN_y state. In spite of the N₂ annealing at a temperature of 950 °C, the N1 intensity of RTNA is similar to that of an RTN film. Combining these data with nitrogen MEIS profiles, it is obvious that the N in the film and interfacial region is stable, even after an RTNA process. According to previous reports, the N2 component at 398.3 eV is related to the N component in the SiO₂ matrix [12]. This indicates that some of the diffused N has reacted with the interfacial SiO₂ as shown previously in the MEIS profiles. N3 and N4 components are considered to be N components in non-stoichiometric SiO_{2-x}N_x and Si₂ON even though it is difficult to precisely determine the peak energy [16,17]. Because the N2, N3 and N4 components are bonded to Si compounds without Hf, they are stable after annealing. The N5 component at about 401.8 eV can be attributed to the presence of SiO₂N states [12,16].

REELS spectra and XPS valence band spectra were also obtained to verify the variation in E_g and the valence band offset (ΔE_v). The change in E_g values was readily observed, as shown in the REELS data of Fig. 3(a). The value of E_g for an as-grown film was 5.34 eV, which is nearly the same as previously reported experimental results and *ab initio* calculations [18–20]. The E_g values are abruptly decreased after the RTN because the occupied N 2p state is closer to the Fermi level than the O 2p state in a HfSiO film [5]. The slight change in E_g value after the RTNA process indicates that the electronic structures of the O and N K edges after RTN and RTNA are both maintained, which are consistent with the absorption spectra shown in Fig. 2. Fig. 3(b) shows XPS spectra for the valence band with respect to the valence band maximum (VBM) for Si and extrapolated onset values, which correspond to the ΔE_v between HfSiO and Si. The ΔE_v value (2.25 eV) of an as-grown film is related to O 2p states in the Hf-based oxide. As shown in Fig. 3(b), after the RTN and RTNA treatments, ΔE_v decreases dramatically to 1.41 eV and 1.42 eV, respectively. As discussed above, these low values are originated from the N 2p state below E_F . Moreover, the absence of any change in the RTNA film compared with the RTN film provides evidence that the electronic structure of N in the nitrated film remains unchanged after RTNA.

The evaluated values of E_g , ΔE_v and the calculated conduction band offsets (ΔE_c) are tabulated in Table 1, where $\Delta E_c = E_g - \Delta E_v - \Delta E_{g, Si}$. An important finding is that, after nitridation (RTN), the magnitude of the decrease in the value of ΔE_c is not as large as that of ΔE_v [21]. However, the values for ΔE_c for the RTNA film are decreased to 0.21 eV, compared to that for the RTN film. This decrement can be attributed to the O vacancy in HfSiON which is located adjacent to Hf and Si sites, because the energy state for the O vacancy is located below the conduction band. Thus, the change in E_g after RTNA can be caused by the formation of an O vacancy as a defect state.

To investigate the role of N incorporation and O vacancies more precisely, *ab-initio* calculations were carried out. Fig. 4(a) shows the calculated total density of states (DOS) and E_g for several HfSiO and HfSiON systems with and without an O vacancy. In the case of the HfSiO system, the value for E_g is estimated to be 4.67 eV, which is lower than the experimentally determined value for the as-grown HfSiO film because the local density approximation (LDA) is underestimated. Hence, the discussion is confined, not to the exact value of E_g

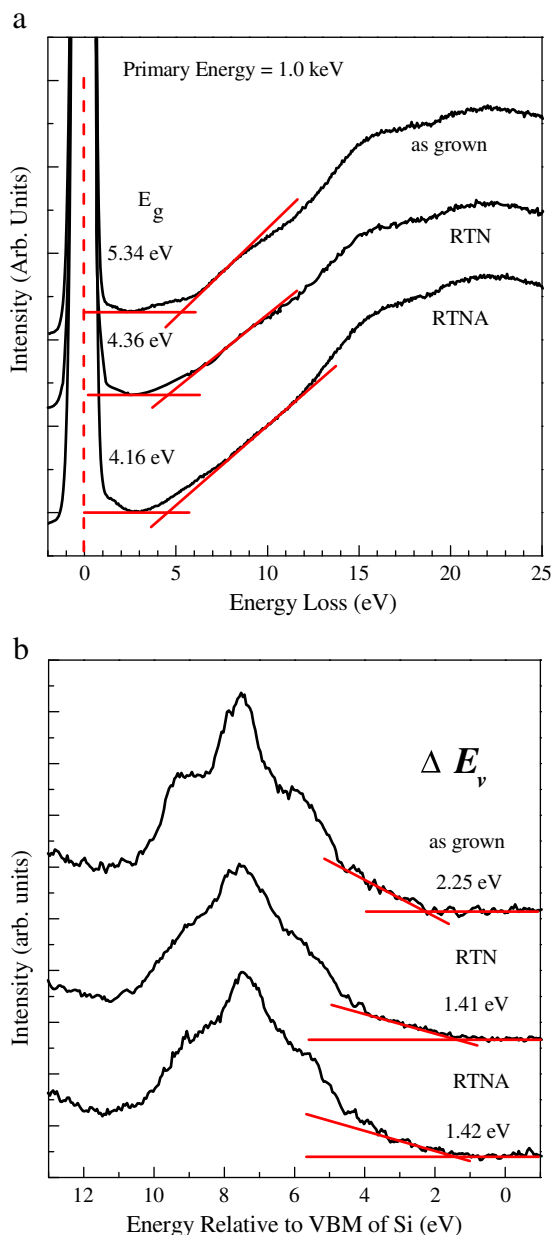


Fig. 3. (a) REELS spectra of as-grown, RTN and RTNA films denoted with E_g values. (b) XPS valence spectra as a function of the energy relative to VBM of Si for as-grown, RTN and RTNA films. Values of ΔE_v are denoted with sample conditions.

but the change in E_g , which is related to N incorporation and the O vacancy in DOS. In the HfSiON system, the E_g is reduced to 3.62 eV which corresponds to the large reduction in E_g in the RTN film. The partial DOS (PDOS) of the HfSiON system (Fig. 4(b)) indicates that the electronic states of N in the valence band are responsible for the reduction of E_g , as discussed above for the experimental results. Considering the O vacancy in the RTNA film, we also estimated the value for E_g in the HfSiON system with an O vacancy. The decrease in the

Table 1
Band gap and band offset for HfSiO films on an as-grown film, an RTN film and an RTNA film.

Energy (eV)	As-grown	RTN	RTNA
E_g	5.34	4.36	4.16
E_v	2.25	1.41	1.42
E_c	1.97	1.83	1.62

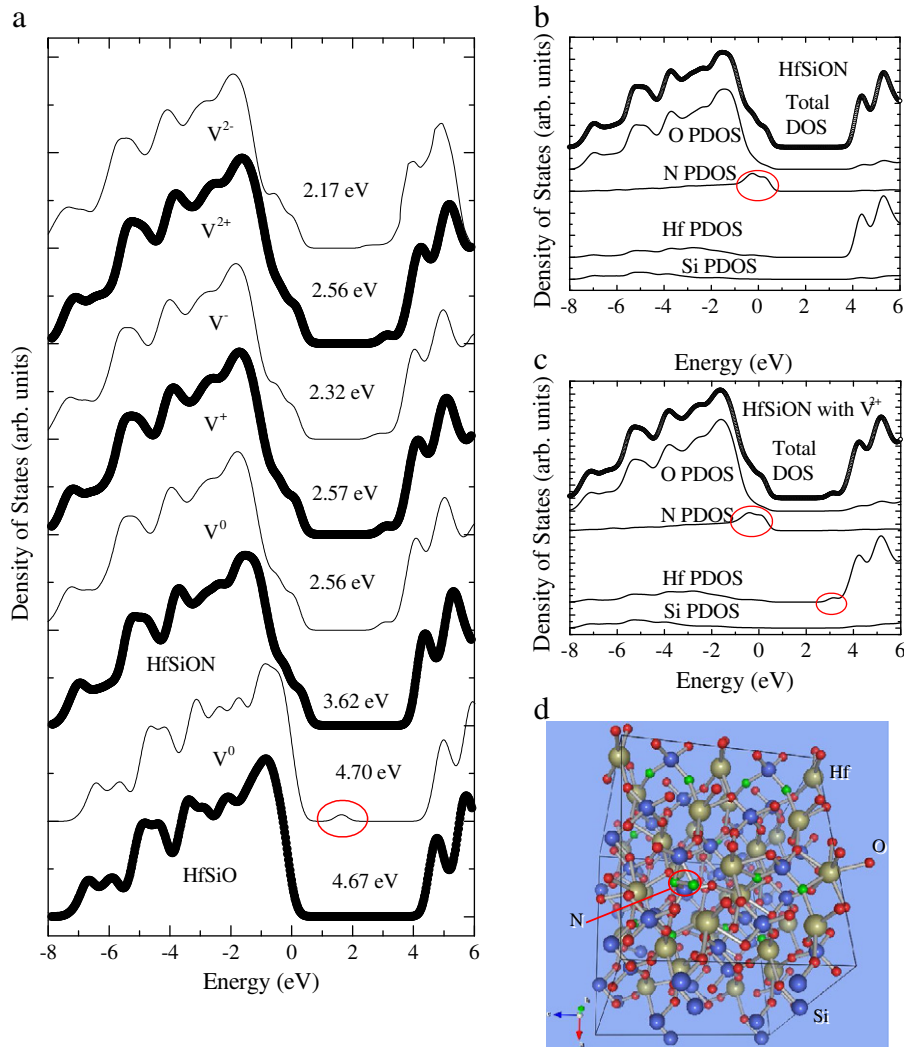


Fig. 4. (a) Total density of states (DOS) in a HfSiO system and a HfSiON system with/without an O vacancy. The two lower spectra are for the HfSiO system and others are for the HfSiON system. The band gap value is also indicated. (b) Partial DOS (PDOS) in HfSiON system without O vacancy. (c) PDOS in HfSiON system with a positively charged O vacancy (V^{2+}). (d) Supercell of the HfSiON system with a positively charged O vacancy (V^+). N atoms that are located next to the O vacancy are indicated as open red circles.

value of E_g is not affected by the charge in the O vacancy (neutral, positively charged and negatively charged), as shown in Fig. 4(a). In addition, the findings indicate that the origin of this change is from the conduction band of the system. The PDOS in the HfSiON system with a positively charged vacancy (V^{2+}) in Fig. 4(c) shows that the lowering of the conduction band offset is related mainly to Hf PDOS as discussed above. However, no evidence was found for the existence of defect states (O vacancy) within the band gap in the HfSiON system (Fig. S2 in Ref. [22]) while the HfSiO system with an O vacancy has a gap-state inside the band gap, as shown in Fig. 4(a). Xiong et al. reported on the formation of a VN_2 complex which consists of two N atoms and an O vacancy in the theoretical results for an N incorporated HfO_2 system [23]. The theoretical results also show that the gap-state is not generated because of the closed shell properties of the VN_2 complex. In the case of a HfSiO system with an O vacancy, as shown in Fig. 4(d) (HfSiO with V^+), the same situation holds. N atoms are paired next to the vacancy and the formed VN_2 complex, as indicated by the open red circles. Therefore, we propose that the absence of a gap-state in the HfSiON system with an O vacancy can be explained by the formation of a VN_2 complex. The absence of a gap state can minimize the electron trap inside the band gap which could subsequently affect the leakage current with Schottky emission.

In summary, the effects of N incorporation and an O vacancy on the electronic state of HfSiO films were investigated. The incorporation of N results in a reduction in E_g and ΔE_v because N 2p states are main constituents of VBM. In addition, the most influential factor for determining the value for ΔE_c is the presence of O vacancies in the RTNA film because of the unoccupied Hf electronic state. The absence of a gap-state within the band gap originates from the VN_2 complex in a HfSiON system with an O vacancy.

Acknowledgment

This work was partially supported by the Joint Program for Samsung Electronics-Yonsei University and the IT R&D program of MKE/KEIT (10035320, "Development of novel 3D stacked devices and core materials for the next generation flash memory"). We gratefully acknowledge the technical advice of K. Chae, C. C. Hwang, and H.-N. Hwang at PAL on beamline 7B1.

Appendix A. Supplementary data

Supplementary data to this article can be found online at <http://dx.doi.org/10.1016/j.susc.2012.04.010>.

References

- [1] M.H. Cho, K.B. Chung, C.N. Whang, D.W. Lee, D.H. Ko, *Appl. Phys. Lett.* 87 (2005) 242906.
- [2] G. Vellianitis, Z.M. Rittersma, J. Petry, *Appl. Phys. Lett.* 89 (2006) 092902.
- [3] S. Kamiyama, T. Miura, Y. Nara, *Electrochem. Solid-State Lett.* 10 (2007) H278.
- [4] G.D. Wilk, R.M. Wallace, J.M. Anthony, *J. Appl. Phys.* 89 (2001) 5243.
- [5] N.T. Barrett, O. Renault, P. Besson, Y.L. Tiec, F. Martin, *Appl. Phys. Lett.* 88 (2006) 162906.
- [6] J.P. Kim, Y.S. Kim, H.J. Lim, J.H. Lee, S.J. Doh, H.S. Jung, S.K. Han, M.J. Kim, J.H. Lee, N.I. Lee, *Tech. Dig. Int. Electron Devices Meet. 2004* (2004) 125.
- [7] A.S. Foster, F.L. Gejo, A.L. Shluger, R.M. Nieminen, *Phys. Rev. B* 65 (2002) 174117.
- [8] K. Xiong, Y. Du, K. Tse, J. Robertson, *J. Appl. Phys.* 101 (2007) 024101.
- [9] G. Kresse, J. Furthmüller, *Phys. Rev. B* 54 (1996) 11169.
- [10] K. Momma, F. Izumi, *J. Appl. Crystallogr.* 41 (2008) 653.
- [11] See supplementary material for the raw data with the fitted results.
- [12] M.H. Cho, K.B. Chung, C.N. Whang, D.H. Ko, J.H. Lee, N.I. Lee, *Appl. Phys. Lett.* 88 (2006) 202902.
- [13] H. Kobayashi, T. Mizokuro, Y. Nakato, K. Yoneda, Y. Todokoro, *Appl. Phys. Lett.* 71 (1997) 1978.
- [14] K.B. Chung, C.N. Whang, M.H. Cho, D.H. Ko, *Appl. Phys. Lett.* 88 (2006) 111913.
- [15] G. Lucovsky, H. Seo, S. Lee, L.B. Fleming, M.D. Ulrich, J. Lüning, P. Lysaght, G. Bersuker, *Jpn. J. Appl. Phys.* 46 (2007) 1899.
- [16] T. Satoshi, O. Jun, T. Haruhiko, O. Masaharu, L. Dong-Ick, S. Shiyu, S. Steven, A.P. Piero, A. Takashi, F. Seiichi, *Appl. Phys. Lett.* 87 (2005) 182908.
- [17] M.H. Cho, K.B. Chung, D.W. Moon, *Appl. Phys. Lett.* 89 (2006) 182908.
- [18] T. Ito, H. Kato, T. Nango, Y. Ohki, *Jpn. J. Appl. Phys.* 43 (2004) 8199.
- [19] I. Nobuyuki, M. Kenzo, *J. Appl. Phys.* 94 (2003) 480.
- [20] T. Hideki, K. Tsu-Jae, *Appl. Phys. Lett.* 83 (2003) 788.
- [21] H. Momida, T. Hamada, T. Yamamoto, T. Uda, N. Umezawa, T. Chikyow, K. Shiraishi, T. Ohno, *Appl. Phys. Lett.* 88 (2006) 112903.
- [22] See supplementary material for the density of states for the HfSiO and HfSiON with or without vacancy.
- [23] K. Xiong, J. Robertson, S.J. Clark, *J. Appl. Phys.* 99 (2006) 044105.